ELSEVIER

Journal of Non-Crystalline Solids 241 (1998) 38–44

JOURNAL OF NON-CRYSTALLINE SOLIDS

Fractal geometry change induced by compression densification

I. Beurroies [a], L. Duffours [a], P. Delord [b], T. Woignier [a], J. Phalippou [a,*]

[a] *Lab. de Science des Mat. Vitreux, Unite de Recherche Associée au CNRS, Case 069 – Place Eugene Bataillon, 34095 Montpellier, France*

[b] *Groupe de Dynamique des Phases Condensées, UMR N° 5581, Université de Montpellier II – Place E. Bataillon, 34095 Montpellier cedex, France*

Received 1 July 1997; received in revised form 6 April 1998

Abstract

Texture change induced by an isostatic compression of low density aerogels exhibiting fractal geometry has been investigated. Fractal features are analyzed from small angle X-ray scattering experiments. It was found that at the onset of densification a decrease in the correlation length occurs while the fractal dimension increases a little. Isostatic compression leads to cluster interpenetration. This provoked solid arm entanglement modifies the fractal range of cluster. For higher pressures correlation length does not change indicating that the cluster size is constant. Further densification has been related to the collapse of pores located between clusters. © 1998 Elsevier Science B.V. All rights reserved.

1. Introduction

It is now well established that the texture of low density silica aerogels may be described using fractal geometry [1,2]. For a porous material the fractal range spans between two limits. The lowest limit of the fractal is obviously the lowest size of the dense matter from which the fractal is built up. The highest limit is related to lengths above which the material enters the homogeneous regime. Additionally, the fractal dimension D quantifies the variation of the mass of solid as a function of observation scale. These fractal features can also be observed in wet gels. They vary according to the silica content [4]. Fractal geometry of aerogels depends on process parameters (temperature, [H_2O] etc...). One of the most sensible is the nature of catalyst (HNO_3 or NH_4OH) used to perform hydrolysis and polycondensation reactions giving rise to the liquid gelation [5]. Several models have been offered to account for the observed fractal D changes with respect to aggregation mechanisms [6,7].

Variation in fractal features requires treatments which, by changing external parameters, induce modifications. According to sintering [8] (taking place by a viscous flow mechanism), a heat treatment provides another route to modify fractal geometry. As sintering proceeds, both the particle size and mean length correlation vary. Such evolution has been previously modelled [9,10].

More recently, several papers pointed out that aerogels can be densified by submitting them under an isostatic pressure [11–14]. This room temperature densification, associated with sample shrinkage, is calculated from the porosimeter

* Corresponding author. Tel.: +33-467 52 59 03; fax: +33-467 54 48 01; e-mail: phalippo@univ-montp2.fr.

0022-3093/98/$ – see front matter © 1998 Elsevier Science B.V. All rights reserved.
PII: S0022-3093(98)00748-0

equipment. The volume shrinkage is obviously related to microstructure evolution. This paper deals with fractal feature changes induced by pressure densification of low density silica aerogels.

2. Experimental

Silica alcogels are prepared using tetramethoxysilane (TMOS) diluted in ethanol. Hydrolysis reaction is carried out using pure water (N samples) or using a 0.01N ammonia solution (B samples). The molar ratio H_2O/TMOS is 4. Aerogels are obtained by a hypercritical drying treatment carried out in an autoclave (305°C, 13 MPa) [15], followed by an oxidation thermal treatment at a temperature of 350°C for 12 h in air. The monolithic aerogel is then sawed to obtain several identical samples. Samples have a cylindrical shape of 20 mm long and 8 mm diameter. The density is calculated by weighting aerogels whose the precise dimensions are mentioned above. The density accuracy is 10^{-2}. Pressure is applied by a mercury porosimeter based on the fact that mercury cannot enter the fine structure of the pores of aerogel. The pressure is then released and the irreversible volume shrinkage is optically measured using a cathetometer. The measurement is directly done on the meniscus oil – mercury through the transparent tube of the dilatometer of the porosimeter. The meniscus displacement, Δl, in the dilatometer tube (1.5 mm diameter) allows one to calculate the volume shrinkage ΔV ($\Delta V = \Delta l \times (\pi/4)(1.5)^2$ in mm^3). The density of compressed samples depends on initial sample density and volume shrinkage. Pressure has been varied between 0.1 and 20 MPa. Sample densities (multiplied by a factor 10^2) are used to label the samples. As an example, B22(c) is a sample prepared under basic conditions. Its density is 0.22 g/cm^3. The letter c between brackets indicates that samples have been compressed while *i* corresponds to the initial uncompressed aerogel. All samples in N series have been obtained from the same oxided aerogel having a density equal to 0.16 g/cm^3 while samples B × c issued to isostatic pressures applied on a base catalysed aerogel of 0.07 g/cm^3 density.

The samples used to perform small angle X-ray scattering (SAXS) experiments are sawed from cylinders. Slices are gently polished to 1.5 mm thickness to avoid multiple scattering phenomenon. SAXS experiments are carried out on the equipment previously described [16]. Scattering curves are desmeared according to the method proposed by Ströbl [17].

3. Results

In Table 1 are listed the bulk densities of the two samples series as a function of applied pressure. SAXS curves are reported in Fig. 1 for a few selected neutral aerogels. Curves are shifted on the intensity scale for clarity. $I(Q)$, and (Q), the wave vector, are plotted on a log–log scale. Curves can

Table 1
Values of pressure applied to densify aerogel sets

	Pressure (MPa)	ρ (g/cm^3)
N16i	0	0.16
N22c	3	0.22
N32c	5	0.32
N38c	10	0.38
N64c	20	0.64
B07i	0	0.07
B09c	0.1	0.09
B11c	0.3	0.11
B20c	0.8	0.2
B23c	1.2	0.23

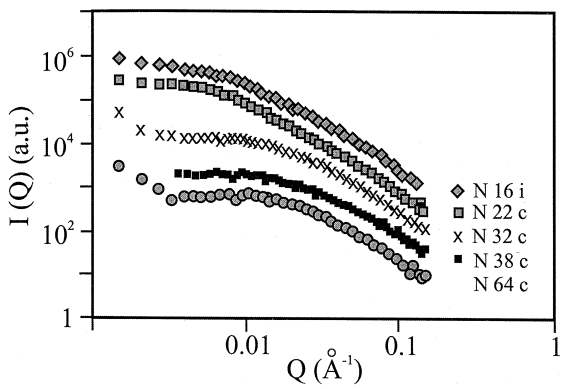

Fig. 1. Selected SAXS curves for neutral aerogels submitted to increasing isostatic pressures.

be divided into different domains. On the side of low wave vector, the curves of the three first densities show a plateau corresponding to the Guinier regime. We must underline that, at very low Q, a little rise in the scattered intensity is observed for a few relatively dense samples. This rise indicates the presence of density variation in the micron range. An analogous intensity increase has been previously reported on aerogels samples subjected to a sintering thermal treatment [5]. It was suggested that inhomogeneities or cracking are responsible for this feature. It is noteworthy that this phenomenon is never observed in non-compacted or non-sintered initially dense aerogels indicating that this phenomenon is not directly related to density increase.

In the Q intermediate range, the fractal regime is observed. It spans between Q values corresponding to $2\pi\xi^{-1}$ and $2\pi a^{-1}$, where ξ is the average correlation length above which the material is no more fractal (ξ may be associated to the average size of the cluster), a, the average particle size below which the material may be considered as fully dense.

Considering an assembly of spherical particles aggregated to form clusters having disordered fractal geometry, the correlation function $G(r)$ is expressed by the relation

$$G(r) \propto \left(\frac{r}{a}\right)^{D-3} e^{-r/\xi}, \tag{1}$$

where D is the fractal dimension. The cut-off on the side of high length scales is described by an exponential function. That permits to give an analytical variation of the scattered intensity as a function of the wave vector [18,19]

$$I(Q) = A\rho^2\xi^2 \frac{\Gamma(D+1)}{(1+q^2\xi^2)^{(D-1)/2}} \frac{\sin(D-1)\arctan(q\xi)}{(D-1)q\xi}, \tag{2}$$

where A is a constant depending on the square of the average scattering length, Γ the gamma function and ρ the bulk density.

Fitting the experimental curve with the calculated one provides an estimate of the fractal dimension and of the average correlation length. This fit applies to the cross-over between Guinier and fractal regimes.

Figs. 2 and 3 show the respective variations of ξ and D as the density of sample increases. As observed, the correlation length first strongly decreases when the density increases up to 0.35 g/cm^3, then it remains constant for higher pressures while density continues to increase. Additionally the fractal dimension does not evolve as a function of the density.

In the high Q domain, a slope change occurs at a value (Q_a) which is proportional to $2\pi/a$. Oxidised neutral reacted silica aerogels obey a classical Porod's law $I(Q) \propto Q^{-4}$ for Q values higher than $2\pi/a$ [2]. The slope change between the fractal domain and the Porod's domain has been used to appreciate the lower fractal cut-off. The accuracy of the measurement mainly depends on the extent

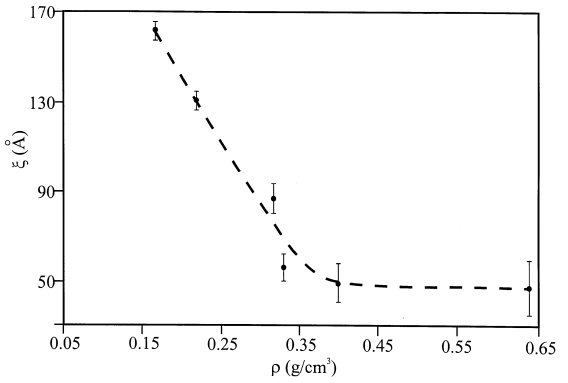

Fig. 2. Variation of the correlation length with the bulk density for initial and compressed neutral silica aerogels (full sample series). Error bars are estimated from the quality of the fit between experimental data and theoretical relationships.

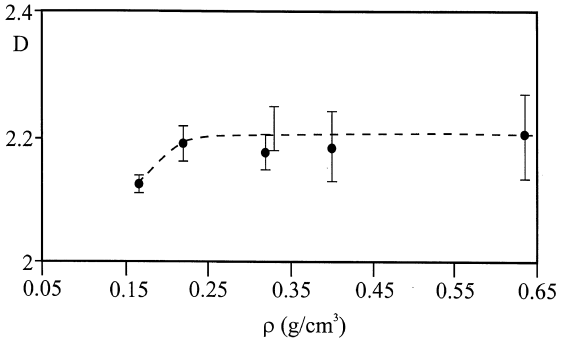

Fig. 3. Variation of fractal dimension with bulk density for initial and compressed neutral silica aerogels.

of the fractal range. The value of a corresponding to aerogels which are fractal on a very narrow range of scales and for which a straight line cannot easily be drawn, is difficult to appreciate. This must be regarded as a rough estimate rather than a precise value. As the densification proceeds, the value a remains constant near 10 Å.

SAXS experiments performed on base catalysed aerogels are shown in Fig. 4. To show fractal geometry, base catalyzed aerogels must have very low density [20]. The sample series is obtained by compressing an aerogel having a starting density of 0.07 g/cm^3. Regime changes are clearly observed. They are indicated by arrows drawn in Fig. 4. However, it was found that, owing to the oxidation treatment and contrarily to neutral reacted aerogels, a slope of −4 is not reached on the high Q side of the curve log $I(Q)$ versus log Q. The slope is equal to −3.2 and remains about constant as the pressure increases. This slope value does not reach −4 value as does aerogel whose density increases by a sintering phenomenon induced by a thermal treatment performed above 800°C [3,9]. Sintering changes the texture at the microscopic scale smoothing the surface, eliminating the micropores. Compression transforms the material at the macroscopic scale but does not modify the microstructure. In addition, on the low Q range, an $I(Q)$ rise is not observed for these base catalyzed aerogels whose the density does not exceed 0.23 g/cm^3.

SAXS curves have been analyzed as mentioned above. Figs. 5 and 6 show the evolution of both the correlation length and volume fractal dimension as a function of sample densities. The correlation length first decreases, then remains constant while density continues to increase. Correlatively, the volume fractal dimension shows a small increase then reaches a plateau value indicating that the fractal geometry no more evolves as the bulk density of the aerogel increases.

During the course of densification, performed by applying higher and higher stresses, the location of the crossover between the volume fractal regime and the surface fractal regime does not shift. The crossover is located at a Q value corresponding to about 14 Å.

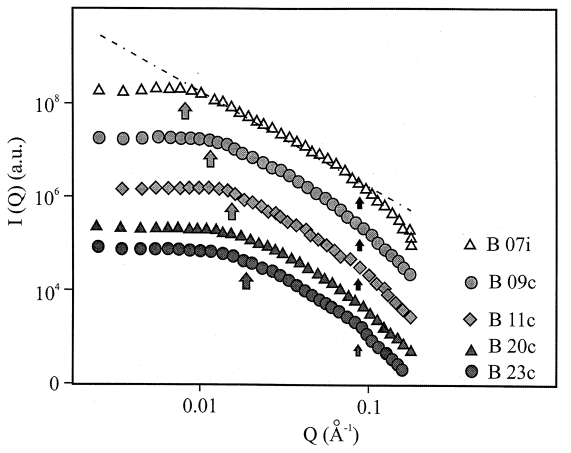

Fig. 4. Selected SAXS of base catalysed silica aerogels. The samples are oxidised and then compressed.

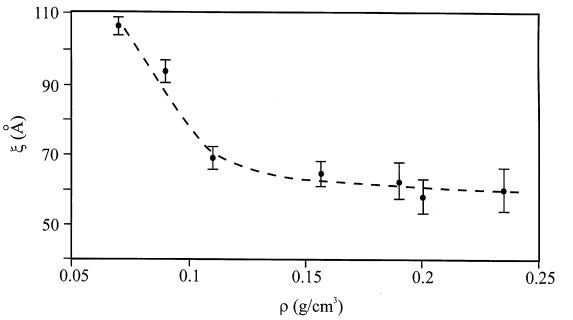

Fig. 5. Variation of the correlation length with the bulk density for initial and compressed base catalysed silica aerogels (full sample series).

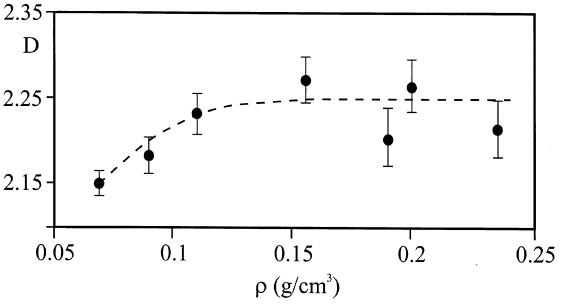

Fig. 6. Variation of fractal dimension with bulk density for initial and compressed base catalyzed silica aerogels.

4. Discussion

A gel forms when fractal clusters aggregate to establish a percolation solid network. It has been already shown [2] that gels obtained by changing the dilution of tetramethoxysilane in alcohol belong to the same family. Each of them is built with clusters having about the same size which mainly depends on monomer species dilution. Unaggregated clusters continue to stick to percolating network well after gelation. Aged gel consists of entangled clusters wetted by the liquid solvent. Hypercritical drying process induces a restructuring phenomenon, as observed from the occurrence of shrinkage [20] and the increase of the fractal dimension [22]. A fractal geometry is characterized by the relation

$$\frac{\rho(\xi)}{\rho(a)} = \left[\frac{\xi}{a}\right]^{D-3}, \tag{3}$$

where $\rho(\xi)$ is the density corresponding to the mean correlation length, ξ, of the fractal material and $\rho(a)$ the density corresponding to the mean particle size, a, of the primary particles. Taking $\rho(a)$ equal to that of silica $\rho(\xi)$ can be estimated.

For neutral aerogels it has been previously demonstrated that a set of samples whose the bulk density varies according to the monomer content of the starting solution are mutually self-similar [2]. The following relation applies:

$$\rho(\xi) \propto \xi^{D-3}. \tag{4}$$

On the other hand, a thermal treatment inducing a sintering allows to densify an initial fractal neutral aerogel. The partially densified aerogel obeys the relation [9]

$$\rho(\xi) \propto \xi^{-3}. \tag{5}$$

Base catalyzed aerogels belong to the same family regarding sintering [10]. We have checked these two mentioned equations to these new aerogels sets for which the density increase is obtained by isostatic pressure.

The slopes of the mean square lines obtained for compressed neutral is −1.03 and that of catalysed is −1.12. Taking a mean value, D, of 2.2 for neutral series, the first equation gives a slope of 0.8 while the second one applied to both series corresponds to a slope −3. Consequently the density increase induced by compression is likely related to a peculiar textural change. We must underline that slopes log $\rho(\xi)$ versus log ξ are not strictly identical for B and N sets. This feature may indicate that the initial aerogel texture, microporous for N set and macroporous for B set may also play a role (Fig. 7).

Experiments performed using SAXS explore the structure of aerogels in the range of clusters. They show that there is a regime change both on the correlation length and fractal dimension as the density increases. In the domain of low pressures, clusters decrease in size while a slight increase in the fractal dimension is observed. The decrease of the size of fractal cluster may be induced by two sorts of mechanisms. The first one consists of an irreversible compaction of clusters without change in the cluster arrangement. The second concerns the possible interpenetration of clusters between them. Obviously these two mechanisms may act together to cause macroscopic aerogel densification.

In the first domain, if we assume that the densification is associated with compaction of individual clusters, the cluster volume, V, decreases and the mass remains constant. Consequently the volume fractal dimension is expected to increase according to

$$m = \text{constant} \propto V^D \xi^{3D}, \tag{6}$$

where m is the mass of cluster and V its volume.

Additionally, since the size of primary particles, a, remains constant (given by SAXS experiments),

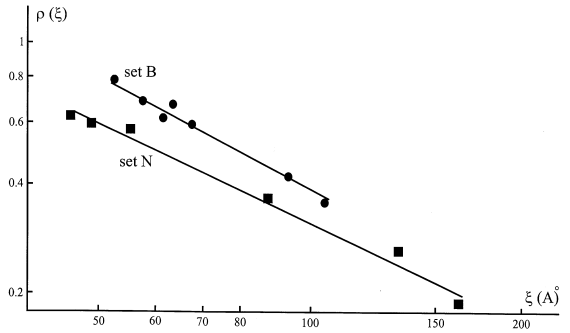

Fig. 7. Variation of $\rho(\xi)$ versus ξ for the two aerogel sets.

there is no collapse or sintering between primary particles. They must be regarded as keeping their individuality. Cluster compression would be due to small changes in particle arrangements. Consequently, the number of balls, N, required to cover the entire volume of solid building up the cluster must remain unchanged [23]. Hence

$$N \propto \left[\frac{\xi}{a}\right]^D = Cte \quad \text{or} \quad \xi \propto a. \tag{7}$$

Since, for the two aerogels sets, ξ decreases while a remains constant, the first domain cannot be associated to a sole compaction effect. An interpenetration of clusters must also occur. Since the value of fractal dimension is higher than 2, clusters. are not mutually transparent [24]. Thus the cluster interpenetration requires buckling and breaking of bonds which initially establish the sticking between clusters. Breaking of a few bonds is also counter-balanced by new bonds formation since the arms of clusters are covered with reactive silanol groups. The more the clusters interpenetrate, the more new bonds are formed. Thus the interpenetration is a limited mechanism. Its extend mainly depends on the cluster structures (like the nature of the catalyst, dilution...), and slightly depends on the applied pressure. The real mechanism allowing the clusters to interpenetrate is difficult to evaluate on the basis of textural properties. Indeed, these two mechanisms are expected to act both on the porous volume and the pore size. Additionally it is worth to notice that textural analyses have been performed on similar aerogels having higher initial densities. The specific surface area remains about constant or slightly increases in the first stages of compression-densification [25]. Owing to compression, breaking of links between clusters leads to an elastic constant decrease. This has been previously demonstrated [16,26].

Obviously, the density increases with the applied pressure. However associated with limited interpenetration of clusters, there is a density, depending on the aerogel nature, beyond which parameters describing the fractal geometry of elementary clusters evolve no more. This corresponds to the second domain. Nevertheless the bulk density continues to increase. This increase must now be associated with arrangement of clusters to form a more packed network. Pores located between clusters vanish while the mean coordination number of cluster increases. Macroscopic elastic properties are likely correlated to cluster connectivity in this density range. They do not seem to depend on the fractal volume dimension as recently proposed [27]. In addition, it is worth noticing that an analogous evolution of elastic properties can be obtained using non-fractal aerogels. Even though fractal parameters of aerogel are not the key parameters accounting for elastic properties, they give information allowing to describe phenomena associated with external parameter change such as the temperature for sintering or the isostatic pressure for ambient compaction. The use of fractal aerogels gives microstructural information which complete previous compaction investigations [11–13].

The comparison between the two aerogel series leads to the conclusion that the range of correlation length evolution is wider for neutrally reacted aerogels than that observed for base catalyzed aerogels. Since the two series were chosen in such a way that they exhibit quite identical fractal dimension, we assume that the main difference must be associated to the size of elementary particles. Base catalyzed aerogels are constituted by relatively large particles. They are rigid since they do not shrink during the hypercritical drying schedule [21]. Neutrally reacted aerogels consist of very fine elementary particles sticked together to form the solid network. In such a case the network must be considered as an entanglement of long flexible chains. They are easily strained when submitted to weak stress. Moreover the limit strain (before rupture) of such chains may reach high values according to distance between nodes. A schematic evolution of an assembly of three schematized and assumed fractal clusters is displayed in Fig. 8.

5. Conclusion

Evolution of fractal parameters during the course of the isostatic compression of aerogels

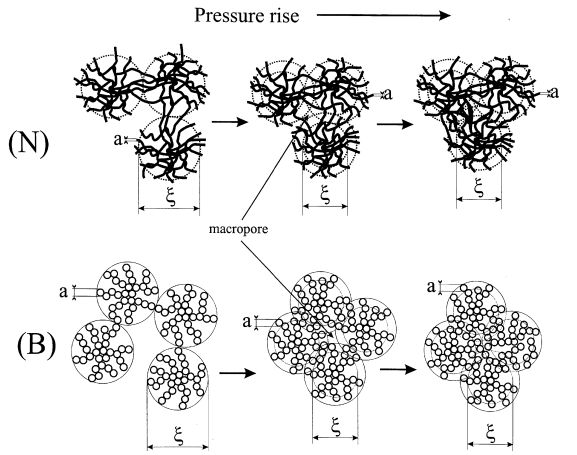

Fig. 8. A schematic assembly of fractal clusters which evolves under increasing isostatic pressures. (N) refers to neutral aerogel, (B) to base catalyzed aerogel.

shows that there are two main regimes as a function of bulk density. At low pressures the external pressure acts on fractal clusters by lowering correlation length and increasing fractal dimension. These two features cannot be associated with simple shrinkage of clusters, an entanglement of clusters must occur. Such an entanglement leads to a lowering of the fractal domain while the lower bound, particle size, remains constant. Entanglement of aggregates is favoured by breaking of bonds. It is restricted by the formation of more and more numerous new bonds resulting from the sticking of arms of interpenetrating clusters.

The second regime has been related to vanishing of pores located between clusters. It results in better packing of clusters. Accordingly, clusters would have a higher average co-ordination number. The crossover between these regimes, on the basis of bulk density, depends on the details of aerogel preparation which are known to playing a very important role on the texture of clusters. With respect to their texture, neutral and basic aerogels exhibit little differences in their behaviour under isostatic pressure.

References

[1] W. Schaefer, K.D. Keefer, Phys. Rev. Lett. 56 (1986) 2199.
[2] R. Vacher, T. Woignier, J. Pelous, E. Courtens, Phys. Rev. B 37 (1988) 6500.
[3] A. Emmerling, J. Fricke, J. Non-Cryst. Solids 145 (1992) 113.
[4] G. Dietler, C. Aubert, D.S. Cannell, P. Wiltzius, Phys. Rev. Lett. 57 (1986) 3117.
[5] D.W. Schaefer, B.J. Olivier, C.S. Ashley, D. Richter, B. Farago, B. Frick, L. Hrubesh, M.J. Van Bommel, G. Long, S. Krueger, J. Non-Cryst. Solids 145 (1992) 105.
[6] P. Meakin, Phys. Rev. Lett. 51 (1983) 1119.
[7] M. Kolb, R. Botet, R. Jullien, Phys. Rev. Lett. 51 (1983) 1123.
[8] A. Emmerling, W. Lenhard, J. Fricke, G.A.L. Van de Vorst, J. Sol–Gel Sci. Tech. 8 (1997) 837.
[9] R. Sempere, D. Bourret, T. Woignier, J. Phalippou, R. Jullien, Phys. Rev. Lett. 71 (1993) 3307.
[10] N. Olivi-Tran, R. Jullien, G.W. Cohen-Solal, Europhys. Lett. 30 (1995) 393.
[11] R. Pirard, S. Blacher, F. Brouers, J.P. Pirard, J. Mater. Res. 10 (1995) 1.
[12] L. Duffours, T. Woignier, J. Phalippou, J. Non-Cryst. Solids 186 (1995) 321.
[13] G.W. Scherer, D.M. Smith, X. Qiu, J. Anderson, J. Non-Cryst. Solids 186 (1995) 316.
[14] L. Duffours, T. Woignier, J. Phalippou, J. Non-Cryst. Solids 194 (1996) 283.
[15] M. Prassas, J. Phalippou, J. Zarzycki, J. Mater. Sci. 19 (1984) 1656.
[16] T. Woignier, L. Duffours, I. Beurroies, J. Phalippou, P. Delord, V. Gibiat, J. Sol–Gel Sci. Tech. 8 (1997) 789.
[17] G.R. Ströbl, Acta Crystallogr. A 26 (1970) 367.
[18] T. Freltof, K.J. Kjems, S.K. Sinha, Phys. Rev. B 33 (1986) 269.
[19] J. Teixera, J. Appl. Cryst. 21 (1988) 781.
[20] T. Woignier, J. Phalippou, R. Vacher, J. Pelous, E. Courtens, J. Non-Cryst. Solids 121 (1990) 198.
[21] H. Hdach, T. Woignier, J. Phalippou, G.W. Scherer, J. Non-Cryst. Solids 121 (1990) 202.
[22] D.W. Schaefer, Rev. Phys. Appl. C 4 (4) (1989) 121.
[23] R. Jullien, N. Olivi-Tran, A. Hasmy, T. Woignier, J. Phalippou, D. Bourret, R. Sempere, J. Non-Cryst. Solids 188 (1995) 1.
[24] B.B. Mandelbrot, The Fractal Geometry of Nature, in: W.H. Freeman (Ed.), New York, 1982.
[25] S. Calas, R. Sempere, J. Non-Cryst. Solids 225 (1998) 215.
[26] J. Gross, R. Goswin, R. Gerlach, J. Fricke, Rev. Phys. Appl. C 24 (4) (1989) 185.
[27] A.P. Roberts, M.A. Knackstedt, Physica A 233 (1996) 848.